COMPUTATIONS OF DROP FORMATION FROM A MICRO CAPILLARY IN CO-FLOWING AMBIENT IMMISCIBLE LIQUID

Shunji Homma, Saitama University, Saitama, JAPAN
Muneyuki Yokotsuka, Saitama University, Saitama, JAPAN
Jiro Koga, Saitama University, Saitama, JAPAN

Introduction

Drops are formed when a liquid is injected from a micro-capillary into another immiscible liquid. The resulting drops are used as emulsions for the production of food, medicine, cosmetics and so on. When the drops are mono-dispersed in micro- or nano- scale size, they are applied to the production of microcapsules. Recently, a technology of the drop formation with a co-flowing ambient fluid has been developed, and the size of the resulting drops by this technology becomes much smaller than the size of the micro-capillary[1].

The mode of the drop formation is categorized into two: dripping and jetting. In dripping mode, the drops break off near the capillary, whereas, in jetting mode, nearly uniform drops are produced at the tip of the jet ejected from the capillary. The diameter of drops in jetting mode is smaller than that in dripping mode. Furthermore the resulting drops produced by jetting mode are monodispersed.

In this study, we simulate numerically the formation of jets and drops from a micro-capillary in co-flowing ambient fluid and examine the transition point from dripping to jetting.

Governing Equations and Numerical Method

Figure 1 shows a schematic of the problem. The dispersed phase of viscosity μ_{in} and density ρ_{in} is injected from a micro-capillary into the co-flowing continuous phase of viscosity μ_{out} and density ρ_{out}. If the two immiscible fluids are incompressible and Newtonian, the governing equations are the continuity equation and the Navier-Stokes equation

$$\nabla \cdot \mathbf{u} = 0 , \tag{1}$$

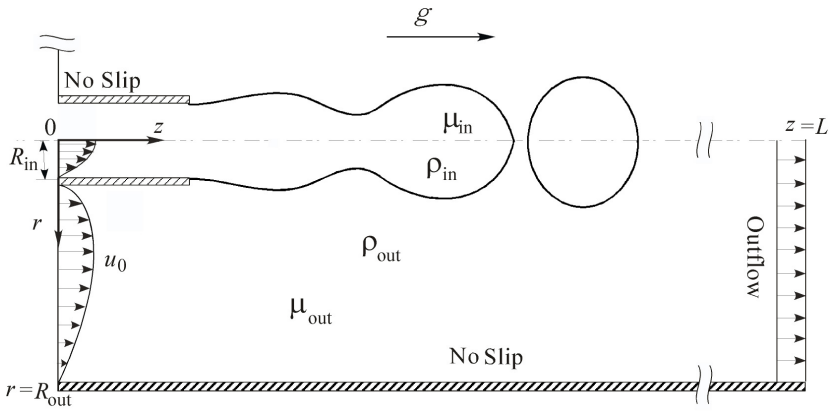

Figure 1. Jet and drop formation from a capillary in co-flowing ambient fluid

$$\frac{\partial}{\partial t}\rho\mathbf{u}+\nabla\cdot\rho\mathbf{u}\mathbf{u}=-\nabla P+\nabla\cdot\mu(\nabla\mathbf{u}+\nabla\mathbf{u}^T)+\rho\mathbf{g}+\int_f\sigma\kappa\mathbf{n}_f\delta(\mathbf{x}-\mathbf{x}_f)dA_f. \tag{2}$$

Eqs. (1) and (2) have been non-dimensionalized by the characteristic scales: the length R_{in} and the velocity u_{in}. Here, R_{in} is the nozzle radius, u_{in} is the average injection velocity of the dispersed phase.

These equations are discretized by finite difference approximations on the two dimensional axisymmetric coordinate and those approximated equations are solved by MAC method. The position of the interface between the dispersed and continuous phases is traced by a Front-Tracking method[2]. The aspect ratio of the computational domain (r:z) is 1:24, and the resolution is 64×1536 determined by grid refinement tests. The boundary conditions are as follows: symmetry on the central axis, outflow on the right, inflow on the left, and no-slip on other boundaries. As the inflow conditions, the velocity distribution of the dispersed phase is given by

$$u_0 = 2 \cdot u_{in} \cdot \left[1-\left(r/R_{in}\right)^2\right] \qquad , 0 \le r \le R_{in} \ , \tag{3}$$

and, that of the continuous phase is given by

$$u_0 = 2 \cdot u_{out} \cdot \left[\frac{\ln\left(1/\alpha\right)}{\ln\left(1/\alpha\right)\cdot(1+\alpha^2)-(1-\alpha^2)}\right] \times\left[1-\left(r/R\right)^2-\frac{1-\alpha^2}{\ln\left(1/\alpha\right)}\cdot\ln\left(R/r\right)\right] \quad , \ R_{in}+R_{th} \le r \le R_{out} \ , \tag{4}$$

where R_{out} is the distance between the central axis and the wall of the capillary, R_{th} is the thickness of the capillary wall, r is the radial coordinate, u_{out} is the average velocity of the continuous phase, and α is the ratio $(R_{in}+R_{th})/R_{out}$.

For numerical simulations, the ratios of the viscosity (μ_{out}/μ_{in}), and the density (ρ_{out}/ρ_{in}) are fixed at 1.5 and 0.8, respectively. The geometry of the nozzle is also fixed as: $R_{out}/R_{in} = 3.0$, $L/R_{in} = 72.0$, and $R_{th}/R_{in} = 0.1$. The ratio of the injection velocities (u_{out}/u_{in}) is varied between 0.03 and 20.0.

Results and Discussion

Figures 2 and **3** show the typical images of drop formation. The values and the definition of the dimensionless numbers are shown in the caption of the figures. When Re and We are small (less than 1), the drops break off near the capillary and satellite drops are formed behind the primary drop (Figure 2). This mode of the drop formation is known as "dripping". As the flow rate of the continuous phase increases ($\mathrm{Re}_{out} = 2.13$), a jet is formed and the drops are produced at the tip of the jet (Figure 3). This mode is called "jetting". The diameter of the drops in jetting mode is smaller than that in dripping mode, and the resulting drops in jetting mode become mono-disperse.

Figure 4 shows the radius of the drop versus the velocity of the continuous phase. The triangle

keys represent the computational results by Hua et. al.[3] The radius decreases with the velocity of the continuous phase. When the velocity of the continuous phase is approximately 9.5, there is a jump in drop radius. This point is the transition from dripping to jetting. The results presented in this study are in close agreement with the ones by Hua et al. [3] The solid line indicates that the predicted radius by linear stability theory. According to the Tomotika's linear stability theory[4], the most unstable wave number is obtained. If a spherical drop is generated with the volume of one wavelength, the corresponding drop radius is given as $R_{drop}= 2.02R_{jet}$. The radius in jetting mode is also in good agreement with the predicted radius by the theory.

Figure 5 shows the transition from dripping to jetting on the diagram of $Ca_{out}(=\mu_{out}u_{out}/\sigma)$ and $We_{in}(= 2R_{in}u_{in}^2\rho_{in}/\sigma)$. These parameters describe, respectively, the magnitude of the viscous shear force from the outer liquid and the magnitude of the inertial force from the inner liquid relative to the surface tension force. If no flow is imposed in the continuous phase, Homma et.al.[5] reported that the jetting mode is obserbed when $We_{in} > 2$. Moreover, Utada et. al.[6] reported that transition boundary is on $Ca_{out} + We_{in} \sim O(1)$ by their experimental study. In Fig. 5, the solid and dashed lines represent the transition boundary for our computational and Utada's results, respectively. In our result, jetting mode is observed when $We_{in} > 0.8$ or $Ca_{out} > 0.1$. This means that a jet forms even low We and Ca, when both the inertial force of the dispersed phase and the drag force of the continuous phase are low. Thus numerical jets are more stable than experimental jets. Since, the jet length is influenced by the disturbances generated at the exit of the capillary we believe that the disturbances generated by our computations are small compared to the experiments. Therefore the computational results show jet formation even lower We_{in} and Ca_{out}.

Figure 2. Drop formation for dripping mode
$[(u_{out}/u_{in}) = 8.8, Re_{in}(=2R_{in}u_{in}\rho_{in}/\mu_{in}) = 0.2, Re_{out}(=2R_{in}u_{out}\rho_{out}/\mu_{out}) = 0.94,$
$We_{in}(=2R_{in}u_{in}^2\rho_{in}/\sigma) = 0.002, We_{out}(=2R_{in}u_{out}^2\rho_{out}/\sigma) = 0.124]$

Figure 3. Drop formation for jetting mode
$[(u_{out}/u_{in}) = 20.0, Re_{in} = 0.2, Re_{out} = 2.13, We_{in} = 0.002, We_{out} = 0.64]$

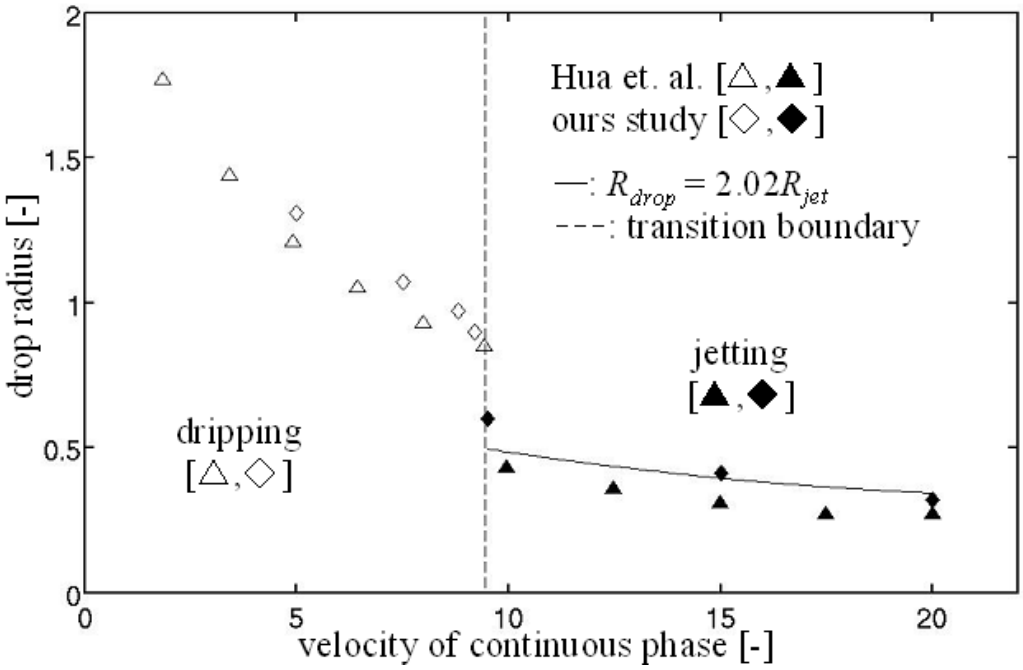

Figure 4. Drop radius versus the velocity of the continuous phase. [Re_{in} = 0.2, We_{in} = 0.002]

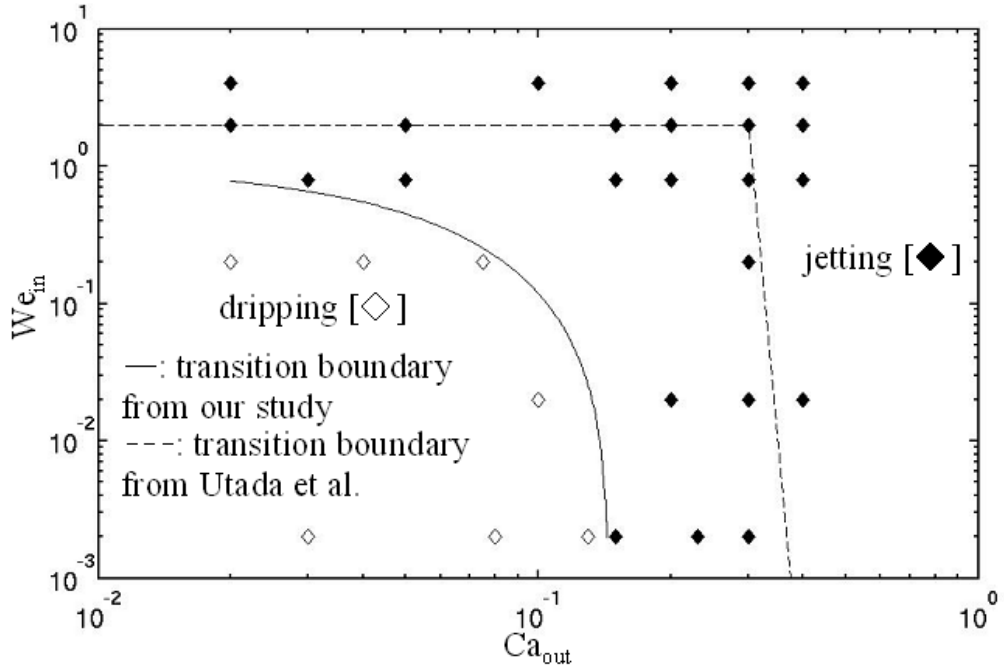

Figure 5. Diagram of the dripping to jetting transition as a function of Ca_{out} and We_{in}

References

1. Cramer, C. *et.al., Chem. Eng. Sci*., vol. 59, pp. 3045-3058 (2004).
2. Unverdi, S. O. and Tryggvason, G., *J. Comput. Phys*., vol. 100, pp. 25-37(1992)
3. Hua, J. *et.al., AIChE J.*, vol. 53, pp. 532534-2547 (2007).
4. Tomotika, S., *Proc. Royal Soc. London* A., vol. 150, pp. 322-337 (1935).
5. Homma, S. *et.al.*, *Chem. Eng. Sci.*, vol. 61, pp. 3986-3996 (2006).
6. Utada, A. S. *et.al.*, *Phys. Rev. Letters.*, vol. 99, 094502 (2007).